SLAC – PUB – 3832
November 1985
(T/E)

RECENT MARK III RESULTS IN RADIATIVE J/ψ DECAYS*

WALTER TOKI

Stanford Linear Accelerator Center
Stanford University, Stanford, CA 94305

representing

The MARK III Collaboration

ABSTRACT

New results on the $\xi(2.2)$ are reported. MarkIII has analyzed new J/ψ data and reconfirmed the $\xi(2.2)$ in radiative J/ψ decays to $K_S^0 K_S^0$ and K^+K^-. The significances of the signals are 3.6 and 4.5 standard deviations, the masses, $2.232 \pm .007 \pm .007$ and $2.230 \pm .006 \pm .014$ GeV/c^2, and the widths, $0.018^{+.023}_{-.015} \pm .010$ and $0.026^{+.020}_{-.016} \pm .017$ GeV/c^2, for the $K_S^0 K_S^0$ and K^+K^- modes, respectively. The branching ratios are $BR(J/\psi \to \gamma\xi, \xi \to K_S^o K_S^o) = (3.2^{+1.6}_{-1.3} \pm 0.7) \times 10^{-5}$ and $BR(J/\psi \to \gamma\xi, \xi \to K^+K^-) = (4.2^{+1.7}_{-1.4} \pm 0.8) \times 10^{-5}$.

Presented at the SLAC Summer Institute on Particle Physics,
Stanford, California, July 29-August 6, 1985

* Work supported in part by the National Science Foundation and by the Department of Energy under contracts DE-AC03-76SF00515, DE-AC02-76ER01195, DE-AC03-81ER40050, and DE-AM03-76SF0034.

1. Review Of The Experimental Situation

The Mark III Collaboration presented evidence for a narrow state, named the ξ, in the summer of 1983.[1] The state was observed in radiative J/ψ decays in the K^+K^- decay channel with a significance of 4.7 standard deviations. There was also slight evidence in the $K^0_S K^0_S$ decay channel with a significance of 2 standard deviations. The mass distributions are displayed in figures 1a and b. The branching ratios, based on a data sample corresponding to 2.7 million produced J/ψ decays, were

$$BR(J/\psi \to \gamma\xi, \xi \to K^+K^-) = (3.8 \pm 1.3 \pm 0.9) \times 10^{-5}$$
$$BR(J/\psi \to \gamma\xi, \xi \to K^0_S K^0_S) = (2.8 \pm 1.4 \pm 0.7) \times 10^{-5}$$

Other modes were searched and several upper limits obtained.[2] They are listed in the following table,

Final State	BR($J/\psi \to \gamma\xi$)·BR($\xi \to$X)
$\xi \to \mu^+\mu^-$	$< 5 \times 10^{-6}$
$\xi \to \pi\pi$	$< 2 \times 10^{-5}$
$\xi \to K^*K$	$< 2.5 \times 10^{-4}$
$\xi \to K^*\bar{K}^*$	$< 3 \times 10^{-4}$
$\xi \to \eta\eta$	$< 7 \times 10^{-5}$
$\xi \to p\bar{p}$	$< 2 \times 10^{-5}$

Before publishing these results it was decided to confirm this state in a new data sample and to increase the statistical significance in the $K^0_S K^0_S$ channel.

About the same time, DM2, the magnetic solenoidal detector at ORSAY, presented new results based on their J/ψ decays. The final results however set upper limits in both the K^+K^- and $K^0_S K^0_S$ modes. Their results, presented in the 1985 Bari Conference, are shown in figures 2a and b.[3] Based on 8 million J/ψ decays they set upper limits, assuming a $\xi(2.2)$ of zero width, of

$$BR(J/\psi \to \gamma\xi, \xi \to K^+K^-) \;<\; 1.2 \times 10^{-5} \text{ at } 95\% \; C.L.$$
$$BR(J/\psi \to \gamma\xi, \xi \to K^0_S K^0_S) \;<\; 2.0 \times 10^{-5} \text{ at } 95\% \; C.L.$$

It is difficult to reconcile these differences. The Mark III and DM2 detectors are similiar although the resolutions and acceptances differ slightly.[4,5] The following table compares the detectors,

Drift,Shower,TOF Counters	Mark III	DM2
D.C. Resolution (1 GeV/c)	21 MeV/c	35 MeV/c
D.C. Acceptance	84%	87%
T.O.F. Resolution	180-230 ps	520 ps
T.O.F. Acceptance	80%	79%
S.C. Resolution	17% $/\sqrt{E}$	19% $/\sqrt{E}$ (to 300 MeV)
S.C. Acceptance	94%	70%

The shower counter resolutions are comparable up to 300 MeV. Above that energy the DM2 shower counter has a resolution of 35% $* E$ because the total radiation length of the counter is insufficient to contain the larger showers. Overall the resolutions of the detectors differ, but the mass resolution after the kinematic constraint fits are very close. The MarkIII detector obtains 10 MeV/c^2 mass resolution (σ) in both modes and DM2 has 12 and 11 MeV/c^2 in the K^+K^- and $K^0_SK^0_S$ modes, respectively.

A large difference between the detectors is in the TOF resolution. The Orsay storage ring, DCI, has a long beam bunch length which causes the time of the beam collision time to be smeared out about ~0.5 ns. Good TOF resolution is important in order to select K^+K^- candidates and reject non-K^+K^- background. This could possibly explain some differences in the K^+K^- results. The $K^0_SK^0_S$ results, however, should be fairly background free and the mass scale can be indirectly checked with the K^0_S mass. The DM2 $K^0_SK^0_S$ mass distribution does not have a signal at 2.22 GeV/c^2 and their upper limit was based on the peak bin in their mass distribution at 2.185 GeV/c^2.

The MarkIII collaboration ran again on the J/ψ resonance from February through May 1985 and collected a data sample that corresponds to 3.1 million produced J/ψ's. This short report will discuss the analysis and results using the complete data sample (2.7+3.1 million produced J/ψ events). It is organized into sections which discuss the analyses of the $K^0_SK^0_S$ and K^+K^- modes, theoretical interpretations and conclusions.

2. $J/\psi \rightarrow \gamma K_S^0 K_S^0$ Analysis

The $\gamma K_S^0 K_S^0$ analysis is based on the full data sample of 5.8 million produced J/ψ events. The initial data reduction has the following requirements:

- Select 4 charged prongs plus one or more neutrals.
- Require 2 distinct sets of $\pi^+\pi^-$ masses to be each within 50 MeV/c^2 of the K_S^0 mass. There are two possible combinations per event.
- Kinematically constrain fit (4-C) to $J/\psi \rightarrow \gamma\pi^+\pi^-\pi^+\pi^-$, using the highest energy gamma in the fit and require the χ^2 fit probability, $P(\chi^2)$, to be greater than 1%.

The momentum used in the kinematic fit is taken at the closest distance of approach of the $\pi^+\pi^-$ tracks. The $\pi^+\pi^-$ mass distribution is shown in figure 3. The K_S^0 mass distribution has a fitted mean of 497 MeV/c^2 and a resolution (σ) of 4.7 MeV/c^2. This agrees with the Monte Carlo resolution. Also the proper decay length is well reproduced by Monte Carlo simulation. Evidence for two K_S^0's in the reaction, $J/\psi \rightarrow \gamma\pi^+\pi^-\pi^+\pi^-$, is shown in figure 4. This figure is a lego plot of one $\pi^+\pi^-$ mass versus the other $\pi^+\pi^-$ mass. There is a clear peak at the $K_S^0 K_S^0$ intersection demonstrating that $J/\psi \rightarrow \gamma K_S^0 K_S^0, K_S^0 \rightarrow \pi^+\pi^-$, is observed.

To extract the $K_S^0 K_S^0$ signal and the background, a new variable,

$$\delta^2 = (m_{\pi_1^+\pi_1^-} - .497)^2 + (m_{\pi_2^+\pi_2^-} - .497)^2$$

is introduced. This represents the distance to the $K_S^0 K_S^0$ center in the $\pi^+\pi^-$ vs. $\pi^+\pi^-$ mass plane. The $\gamma K_S^0 K_S^0$ signal is selected when $\delta^2 < .0004$ (GeV/c^2)^2 or (20 MeV/c^2)^2. The background sample of events have larger values of δ^2. To normalize the background the differential of δ^2 of the signal area should equal that of the control background. The background sample is selected from events satisfying $.0008 < \delta^2 < .0012$ (GeV/c^2)^2. The $K_S^0 K_S^0$ mass distribution is shown for the signal events and the background events in figure 5b. The background events are cross hatched in the figure.

The ξ signal appears superimposed over a broad structure. The non-$K_S^0 K_S^0$ background is very small and estimated to be 9 events in the 2.0 - 2.5 GeV/c^2 $K_S^0 K_S^0$ mass region. The ξ signal in the mass distribution is fitted with a Breit-Wigner function convoluted with a gaussian mass resolution over a smooth background. The monte carlo determined mass resolution was 10 MeV/c^2. The mass and width are determined using an unbinned maximum likelihood fit over all the events. The mass and width are allowed to vary and the mass resolution is fixed in the fit. The results are

$$\mathrm{m}(\xi \rightarrow \mathrm{K_S^0 K_S^0}) = 2.232 \pm .007 \pm .007 \ \ \mathrm{GeV/c^2}$$
$$\Gamma(\xi \rightarrow \mathrm{K_S^0 K_S^0}) = 0.018^{+.023}_{-.015} \pm .010 \ \ \mathrm{GeV/c^2}$$

The statistical significance is 3.6 standard deviations. It is obtained by calculating the maximum likelihood with no signal and comparing the maximum likelihood with a signal where the width and mean are allowed to vary.

The fit yields 23 events. The Monte Carlo efficiency is 28% (not including the $K_S^0 \rightarrow \pi^+\pi^-$ branching ratio) and does not change with the different spin assumptions. The branching ratio is,

$$BR(J/\psi \rightarrow \gamma\xi, \xi \rightarrow K_S^0 K_S^0) = (3.2^{+1.6}_{-1.3} \pm 0.7) \times 10^{-5}$$

The Dalitz plot is displayed in Figure 6b. The diagonal lines are the f', θ and ξ. The f' is peaked near the edge of the Dalitz plot whereas the θ is distributed along the diagonal. The region between the θ and the ξ appears to be peaked near the edge of the Dalitz plot which may indicate its preference for high spin. The ξ appears in the middle and near the edge of the Dalitz plot. The region above the ξ appears to be uniformly distributed in the Dalitz plot.

3. $J/\psi \rightarrow \gamma K^+K^-$ Analysis

The γK^+K^- analysis is performed on the full data sample of 5.8×10^6 produced J/ψ events. The initial data sample is reduced with the following criteria:

- Select 2 charged prongs plus one or more neutrals.
- Kinematically constrain fit (4-C) to $J/\psi \rightarrow \gamma K^+K^-$ using the highest energy gamma in the fit and require the fit to have $P(\chi^2) > 1\%$.

The event sample after these cuts has large backgrounds from $J/\psi \rightarrow \gamma e^+e^-$ and $\gamma\pi^+\pi^-$. These backgrounds are reduced by requiring TOF identification on both tracks. The following variable,

$$\Delta = T_+ \quad - \left(\frac{t_{\pi+} + t_{K+}}{2}\right) \; + \; T_- \quad - \left(\frac{t_{\pi-} + t_{K-}}{2}\right)$$

is defined where $T_\pm$ is the measured times for the $\pm$ tracks and $t_{\pi\pm}$ and $t_{k\pm}$ are the predicted times for the $\pi^\pm$ and $K^\pm$ mass hypotheses. This variable is the difference between the measured times and the mean time of the π and K mass hypotheses. For larger values of Δ, the e^+e^- and $\pi^+\pi^-$ background is reduced because the $K^\pm$ tracks will have longer times. The events are required to have $\Delta > 100\ ps$. This requirement, studied by Monte Carlo, is independent of the K^+K^- mass. Figure 7 shows the resulting efficiency with these cuts as a function of K^+K^- mass. This is a mass plot of reconstructed monte carlo events that were generated with a flat mass distribution.

Backgrounds from $J/\psi \rightarrow \pi^0\pi^+\pi^-$ and $J/\psi \rightarrow \pi^0K^+K^-$ are reduced by examining the fits to the specific background mode. If events have 2 or more γ's they are kinematically fit to $J/\psi \rightarrow \gamma\gamma\pi^+\pi^-$ or $J/\psi \rightarrow \gamma\gamma K^+K^-$. They are rejected if the fit has $P(\chi^2) > 2\%$ and if the $\gamma\gamma$ mass is within 50 MeV/c^2 of the π^0 mass. Figure 5a shows the K^+K^- mass distribution.

These cuts are less restrictive then the cuts used in an earlier analysis. They were used because the new data set had several detector problems. The drift chamber suffered a short in the outermost 3 layers (out of 34 layers) and was operated with only 31 layers for most of the run. This degraded the drift chamber momentum resolution (σ) on dimuons from 35 to 65 MeV/c. The TOF counters resolution (σ) also degraded from 180 ps to 220 ps. This was partially due to beam bunch lengthening which was caused by the mini$-\beta$ magnet modifications at SPEAR in the Summer of 1984. The data using the same cuts is displayed in figures 8a and b for the 1982-83 data set and the 1985 set. The ξ appears clearly in both sets. All results are obtained using both data sets.

Because the new cuts have a larger acceptance, 38%, and do not depend significantly on the spin, more background is present. The backgrounds in the 1.9-2.6 GeV/c^2 K^+K^- mass region are large and difficult to reduce without affecting the signal. The Dalitz plot is shown in Figure 6a. The backgrounds that appear in the Dalitz plot are from $J/\psi \rightarrow K^*K$ and γe^+e^-. The K^*K backgrounds appear as a vertical and horizontal bar at $mass^2(\gamma K^\pm) \simeq .79$ (GeV/c^2)^2. The γe^+e^- background appears at the edge of the Dalitz plot.

To check that the ξ events are not due to these backgrounds the events were studied with cuts on the Dalitz plot. After removing these backgrounds by cutting out the regions $.7 < mass^2(\gamma K^\pm) < .9$ (GeV/c^2)^2 ,to exclude the KK^* background, and $|cos(\theta_{\gamma K})| > 0.99$,to exclude the γe^+e^- backgrounds, the significance of the ξ is slightly reduced. Figure 9 is the resulting K^+K^- mass distribution after these Dalitz plot cuts. Cuts near the edge of the Dalitz are potentially dangerous, especially if the signal events are high spin.

The K^+K^- mass distribution was fitted with a Breit-Wigner function convoluted with a gaussian and a smooth background in the 1.9-2.6 GeV/c^2 mass region.

The mass resolution (σ) after the kinematic constraint (4-C) fit was 10 MeV/c^2. A maximum likelihood fit varying the mass and width and fixing the mass resolution yielded a mass and width of

$$m(\xi \rightarrow K^+K^-) = 2.230 \pm .006 \pm .014 \qquad \mathrm{GeV/c^2}$$
$$\Gamma(\xi \rightarrow K^+K^-) = 0.026^{+.020}_{-.016} \pm .017 \qquad \mathrm{GeV/c^2}$$

The fit obtained 93 signal events and a statistical significance of 4.5 standard deviations. The statistical significance was obtained by comparing the difference in the maximum likelihood fit with and without the signal over a smooth background. The acceptance as determined by Monte Carlo was 38%. The resulting product branching ratio is

$$BR(J/\psi \rightarrow \gamma\xi, \xi \rightarrow K^+K^-) = (4.2^{+1.7}_{-1.4} \ \pm\ 0.8) \times 10^{-5}$$

The first error is from the fit and second error is the systematic error determined from uncertainties is the fit procedure, event selection and flux estimates.

4. Theoretical Interpretations of the ξ

There have been several theoretical interpretations since the evidence for the ξ was first presented. The ξ was interpreted among others as:

1) Higgs Boson

2) High spin $s\bar{s}$ meson

3) Glueball or hybrid (gluon-quark-quark) state.

Before summarizing these general ideas, the possible quantum numbers of the ξ will be briefly discussed.

The spin-parity of the system can be understood by recalling the explanation for the $P\bar{P}$ annihilation experiments to 2 neutral kaons.[6] Since the ξ is seen in a radiative J/ψ decays the C-parity is +1. A $K\bar{K}$ state will be in a definite CP state of ±1 when the wave function is $K_a^0\bar{K}_b^0 \pm K_b^0\bar{K}_a^0$, where a and b refer to the space indices. This state will be observed as $K_{Sa}^0K_{Sb}^0 - K_{La}^0K_{Lb}^0$ for CP=+1 and $K_{La}^0K_{Sb}^0 - K_{Sa}^0K_{Lb}^0$ for CP=-1. Observing the ξ in the $K_S^0K_S^0$ mode restricts it to CP=+1. Hence C=+1 and CP=+1 and consequently P=+1. Since P=$(-1)^J$ for decays to two pseudoscalars, J is even. Summarizing, the ξ must have $J^{PC} = (even)^{++}$.

Assuming that isospin is conserved in its production, the ξ should be an isoscalar. An isoscalar $K\bar{K}$ state should decay equally into K^+K^- and $K^0\bar{K}^0$. Thus the K^+K^- rate should be twice the $K_S^0K_S^0$ rate. The experimental ratio is 1.3±0.8 ± 0.4 which is consistent with the isoscalar hypothesis.

The single Higgs doublet interpretation follows from a paper by Wilczek.[7] The model predicted a vector meson composed of heavy quarks could radiatively decay to a Higgs boson, which would decay to lepton pairs or to heavy quark pairs. Both the width and spin would be zero. Calculation of the Feynman diagrams predict a partial rate of

$$\frac{\Gamma(J/\psi \to \gamma H^0)}{\Gamma(J/\psi \to \mu^+\mu^-)} = \frac{G_F\ m_{J/\psi}^2}{4\sqrt{2}\pi\alpha}\left(1 - \frac{m_H^2}{m_{J/\psi}^2}\right).$$

This model has several difficulties. The predicted rate is BR$(J/\psi \to \gamma H^0) \simeq 3 \cdot 10^{-5}$ and the observed rate to $K\bar{K}$ alone is about 10^{-4}. The model also predicts a rate to $\mu^+\mu^-$ of roughly $1/3(M_\mu/M_s)^2$ times the rate to $K\bar{K}$. Using a value of .5 GeV/c^2 for the strange quark mass, the predicted rate is BR$(J/\psi \to \gamma H^0, H^0 \to \mu^+\mu^-) \simeq 10^{-5}$ which is about a factor 2 larger then our present limit for the ξ decay to mu-pairs.

It has been suggested that the single Higgs doublet model may be modified to have 2 or more doublets.[8,9] The 2 Higgs doublets models, where each doublet couples to a u and d quark separately, can produce a large J/ψ rate and a suppression of the dimuon rate. These models can be arranged to enhance or diminish the production of the Higgs boson in radiative Υ decays. Consequently, the current published limit from CLEO, $B(\Upsilon(1s) \rightarrow \xi, \xi \rightarrow K^+K^-) < 2 \times 10^{-4}$, can not rule out all the models.[10]

The $s\bar{s}$ state interpretation has been developed in a model with $l = 3$ and $s = 1$, where the $s\bar{s}$ quarks form a triplet.[11] This otherwise prosaic interpretation is unusual because the width could narrow (30-50 MeV/c^2) which is atypical for high spin mesons. The model predicts two $s\bar{s}$ states, $^3F_2$ and $^4F_4$, that have few decay modes available and are relatively weak, causing them to be narrow. The prediction includes large decay rates to K^*K, K^*K^*, $\eta\eta$ and $\eta\eta'$. Additionally, the model predicts a ω-like $^3F_2$ partner with a mass about 200 MeV/c^2 lighter. This should be seen in radiative J/ψ decays and be observable in the $\pi\pi$ mode. A large bump in this mode is infact seen both by MarkIII and DM2 around 2.1 GeV/c^2. However, the spin is unknown and it could be the h(2030) which is the spin 4 meson.

The glueball/hybrid interpretation also has been developed in several models. It was pointed out that in the bag model, TM gluons may couple preferentially to $s\bar{s}$.[12] This explained why many new particles seen in radiative J/ψ decays have kaon and η secondaries and also why flavor symmetry seems to fail. This model identified the ξ as a 2^{++} hybrid state and predicts decays to $K^*\bar{K}^*$ and $\Phi\omega$. Other interpretations include identification as a bound state of 2 TM gluons and 3 TE gluons.[13,14]

5. Summary

The Mark III results on the decays $J/\psi \to \gamma\xi, \xi \to K_S^0 K_S^0$ and K^+K^- are summarized in the following table.

	K^+K^-	$K_S^0 K_S^0$
B.R.	$(4.2^{+1.7}_{-1.4} \pm 0.8) \times 10^{-5}$	$(3.2^{+1.6}_{-1.3} \pm 0.7) \times 10^{-5}$
mass	$2.230 \pm .006 \pm .014$ GeV/c^2	$2.232 \pm .007 \pm .007$ GeV/c^2
Γ	$0.026^{+.020}_{-.016} \pm .017$ GeV/c^2	$0.018^{+.023}_{-.015} \pm .010$ GeV/c^2

These results are in disagreement with those of DM2. These differences are not yet understood and may eventually be resolved by confirmation in another mode or from another machine such as LEAR ($P\bar{P} \to \xi \to K_S^0 K_S^0, K^+K^-$).

Future MarkIII plans include a search for other decay modes if the ξ and a measurement of the spin and width in the present data sample of $5.8 \cdot 10^6$ produced J/ψ's. The main approach is to look for J/ψ radiative decays into 2 body states with $s\bar{s}$ content such as K*K, K*K*, $\eta\eta$, $\eta\eta'$, $\eta'\eta'$, $\phi\phi$ and $\phi\omega$. If the ξ has a branching fraction to one of these modes at least comparable to its rate to $K\bar{K}$ there may be a chance to see it if there is little background. Finding any new mode could not only help to confirm it's existence but also isolate some of the theoretical models.

The spin of the ξ will be examined in the $K_S^0 K_S^0$ mode which is relatively background free. Also a 3 pseudoscalar decay mode will be searched for because the scalar spin-parity would be ruled out since a 0^{++} state cannot decay into 3 pseudoscalars. If a three pseudoscalar decay is found this will rule out Higgs models. If the state is higher spin, the width is important to measure because high spin $s\bar{s}$ models predict widths of 30-50 MeV/c^2. A narrow state could rule out these models.

References

1. K. Einsweiler, SLAC-PUB-3202, Sept 1983.

   W. Toki, SLAC-PUB-3262, Nov 1983.

   D. Hitlin, Proceedings of the 1983 International Symposium on Lepton and Photon Interations at High Energies, ed. D. Cassel and D. Kreinick, (Lab. of Nuclear Studies, Cornell University, Ithaca, New York).
2. K. Einsweiler, SLAC-272, May 1984, Ph.D. thesis, unpublished.
3. J. Augustin *et al.*, contributed paper to the International Symposium of Lepton and Photon Interaction at High Energy, Kyoto, Aug 19-24, 1985, preprint LAL 85/27.
4. D. Bernstein *et al.*, , Nucl. Instr. Meth. **226**, 301 (1984).
5. J. Augustin *et al.*, , Physica Scripta **23**, 623 (1981).
6. J. Vandermeulen, Kinematics and Multiparticle Systems,ed. M. Nikolic, (Gordon and Breach,1968).
7. F. Wilczek, Phys. Rev. Lett. **39**, 1304 (1977).
8. R. Barnett, G. Senjanovic, D. Wyler, Phys. Rev. **D30**, 1529 (1984).
9. H. Haber, G. Kane, Phys. Lett. **135**, 196 (1984).
10. S. Behrends *et al.*, Phys. Lett. **137 B**, 277 (1984).
11. S. Godfrey, R. Kokoski, N. Isgur, Phys. Lett. **141 B**, 439 (1984).
12. M. Chanowitz, S. Sharpe, Phys. Lett. **132 B**, 413 (1983).
13. B. Ward, Phys. Rev. **D31**, 2849 (1985).
14. K. Senba and M. Tanimoto, preprint EHU-84-01, January 1984.

Figure Captions

1. $K\bar{K}$ invariant mass distributions of the 1982 and 1983 data for the (a) K^+K^- final state and (b) the $K^0_SK^0_S$ final state.
2. $K\bar{K}$ invariant mass distributions from DM2 for the (a) K^+K^- final state and (b) the $K^0_SK^0_S$ final state.
3. $\pi^+\pi^-$ invariant mass distribution from the reaction $J/\psi \to \gamma\pi^+\pi^-\pi^+\pi^-$.
4. Lego plot of the $\pi^+\pi^-$ invariant mass versus the other $\pi^+\pi^-$ invariant mass in the reaction $J/\psi \to \gamma\pi^+\pi^-\pi^+\pi^-$.
5. $K\bar{K}$ invariant mass distributions of the combined 1982, 1983 and 1985 data sets for the (a) K^+K^- final state and (b) the $K^0_SK^0_S$ final state. The background events are cross hatched.
6. Dalitz plots for (a) the K^+K^- channel and (b) the $K^0_SK^0_S$ channel.
7. Monte carlo efficiency to detect and reconstruct $J/\psi \to \gamma K^+K^-$ events as a function of K^+K^- mass.
8. K^+K^- invariant mass distributions for (a) the 1982 and 1983 ($2.7 \cdot 10^6$ produced J/ψ's) sample and (b) the 1985 ($3.1 \cdot 10^6$ produced J/ψ's) sample.
9. K^+K^- invariant mass distribution after Dalitz plot cuts.

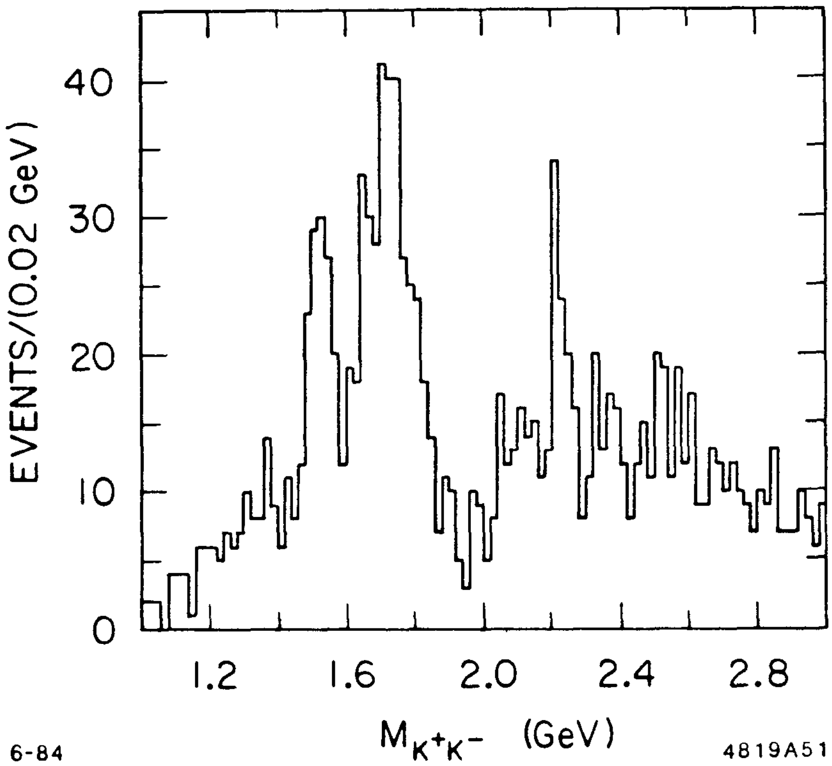

Fig. 1a

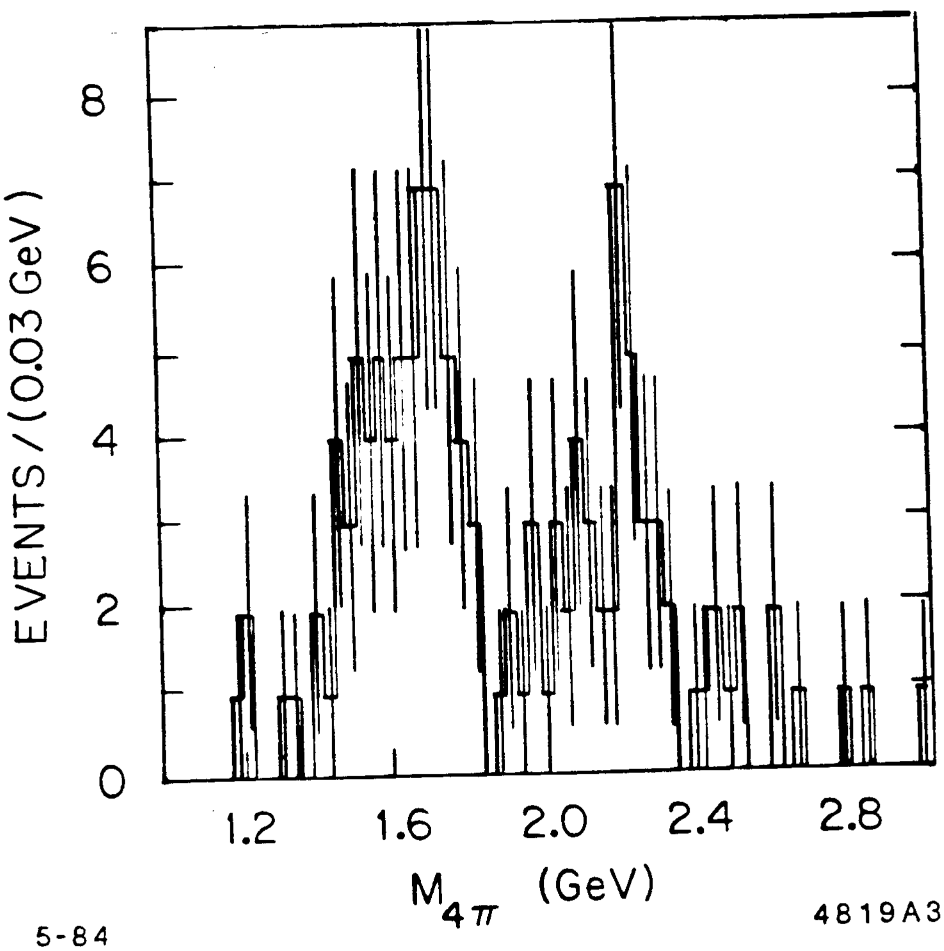

Fig. 1b

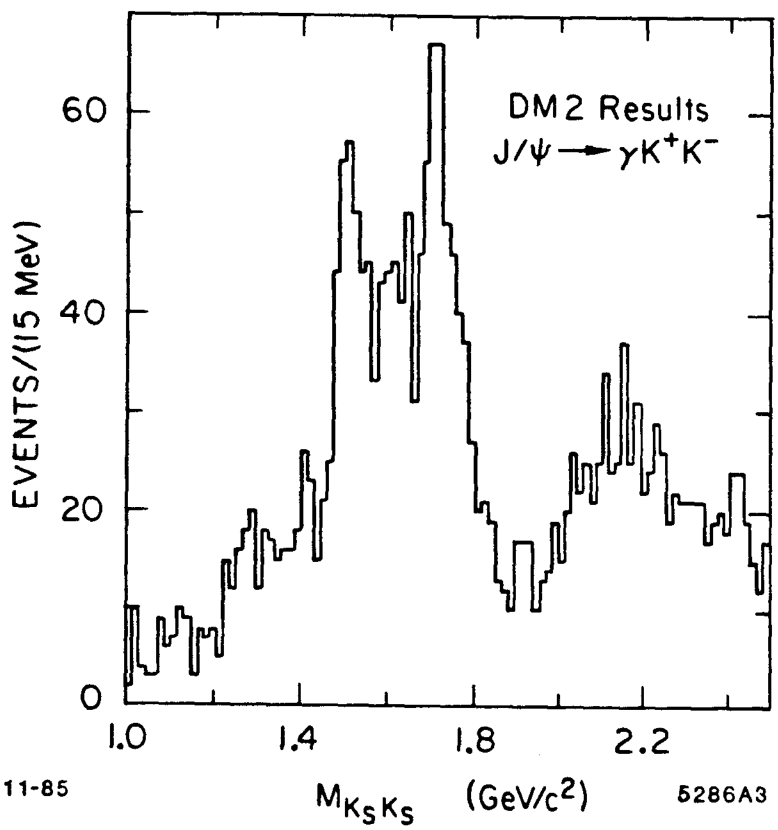

DM2 Results
J/ψ → γK+K−
EVENTS/(15 MeV)
60
40
20
0
1.0
1.4
1.8
2.2
11-85
$M_{K_S K_S}$ (GeV/c²)
5286A3

Fig. 2a

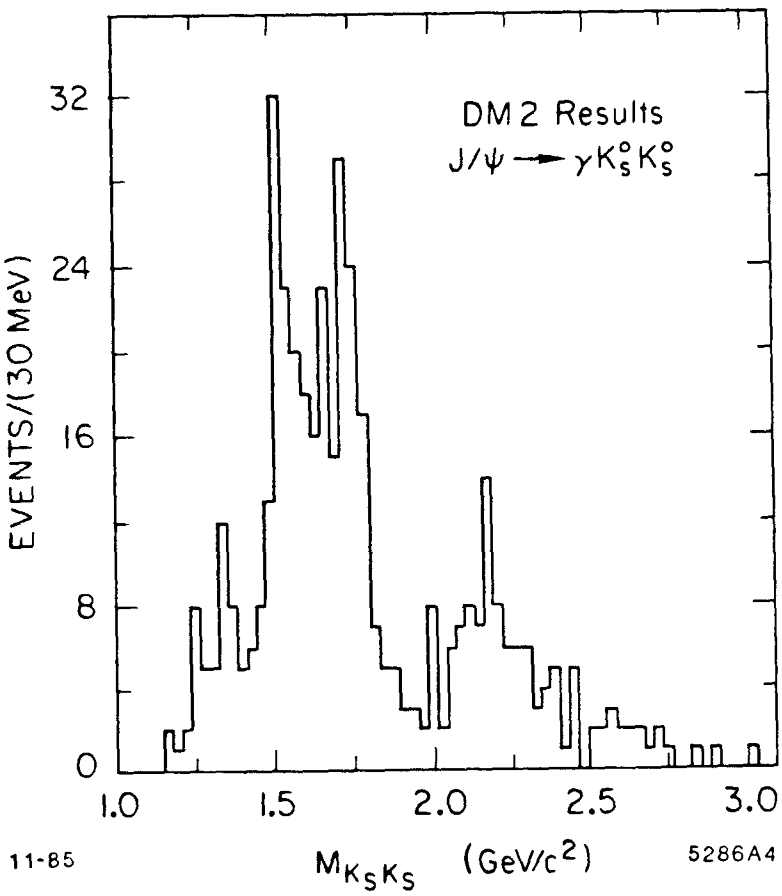
DM 2 Results
J/ψ → γK°s K°s
EVENTS/(30 MeV)
32
24
16
8
0
1.0
1.5
2.0
2.5
3.0
11-85
M_KsKs (GeV/c²)
5286A4

Fig. 2b

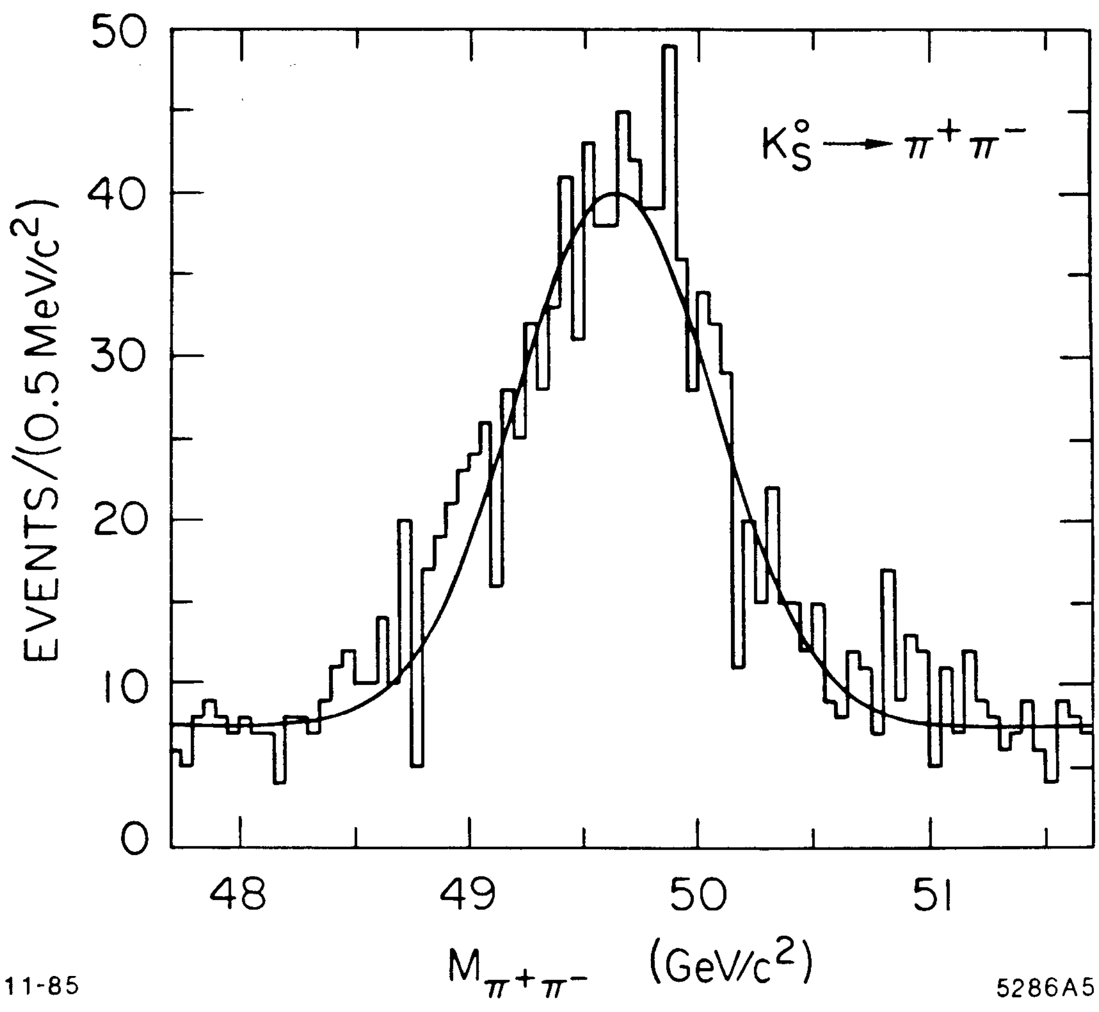
50
40
30
20
10
0
EVENTS/(0.5 MeV/c2)
Ks° → π+π−
48
49
50
51
Mπ+π− (GeV/c2)
11-85
5286A5

Fig. 3

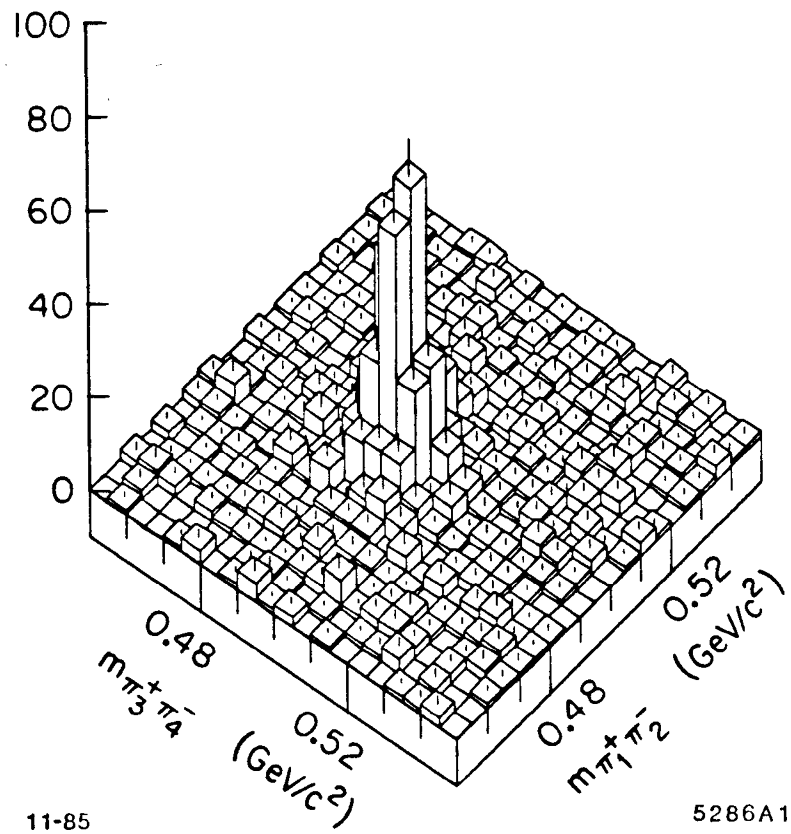

Fig. 4

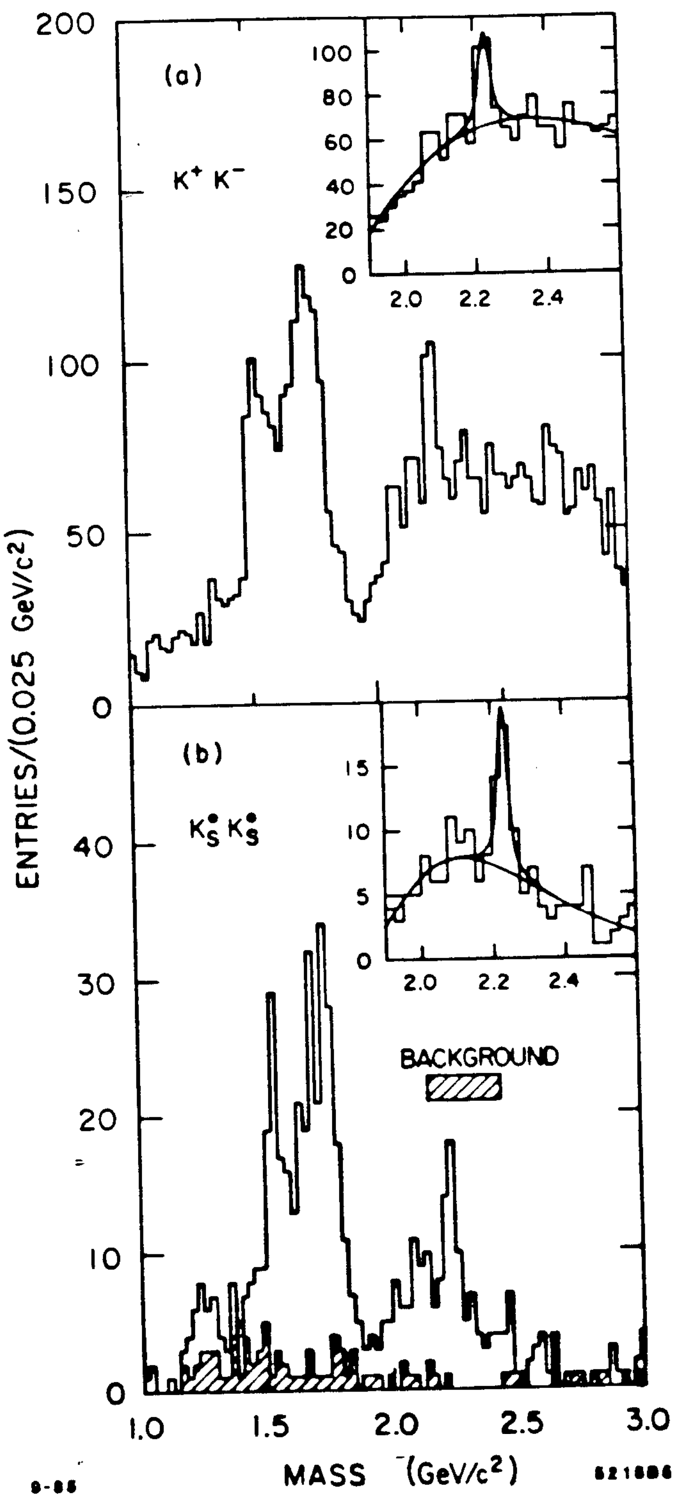

(a)
K⁺ K⁻
(b)
$K_S^0 K_S^0$
BACKGROUND
ENTRIES/(0.025 GeV/c²)
MASS (GeV/c²)
9-85
5218B6

Fig. 5

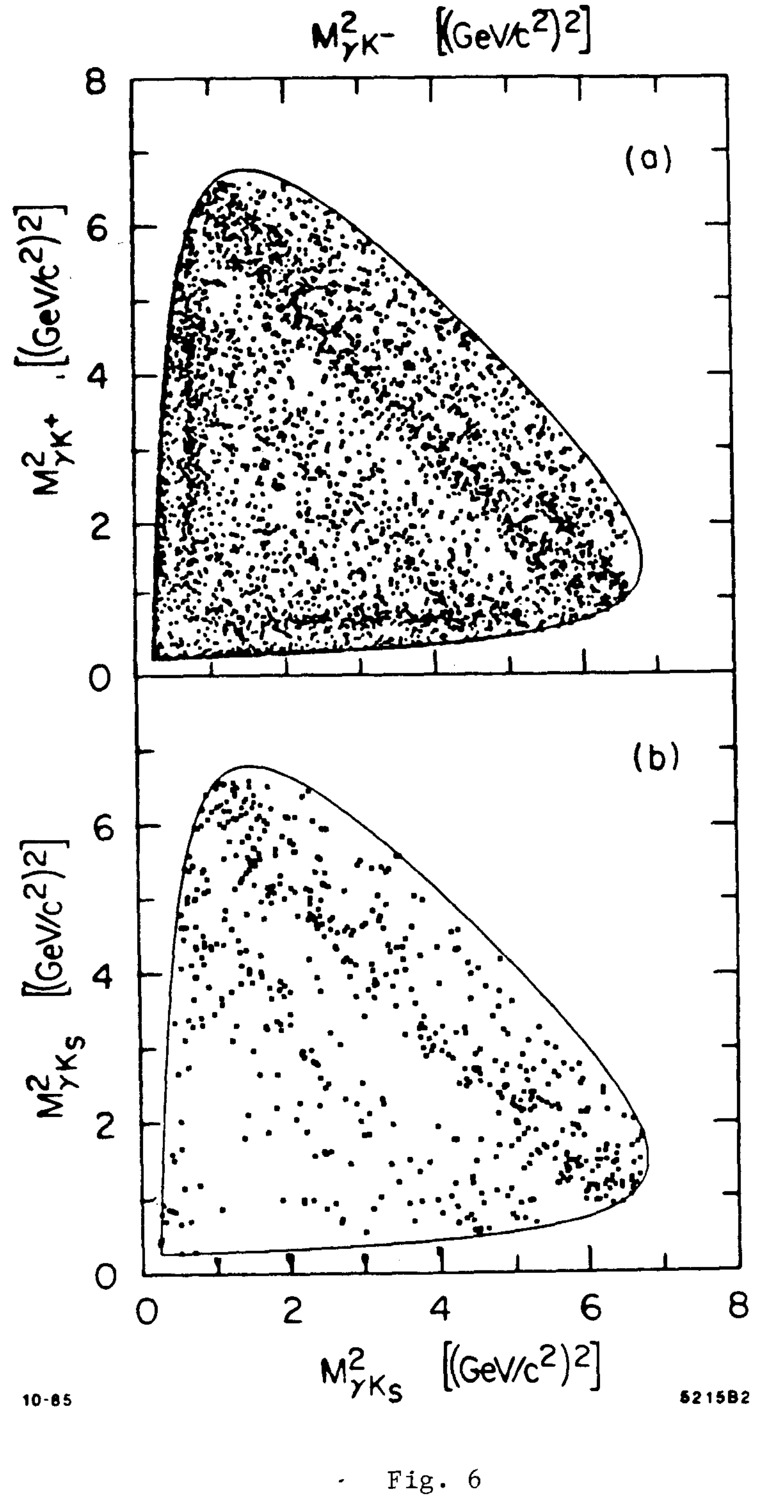
M²γK⁻ [(GeV/c²)²]
(a)
M²γK⁺ [(GeV/c²)²]
(b)
M²γKs [(GeV/c²)²]
0
2
4
6
8
M²γKs [(GeV/c²)²]
10-85
5215B2

Fig. 6

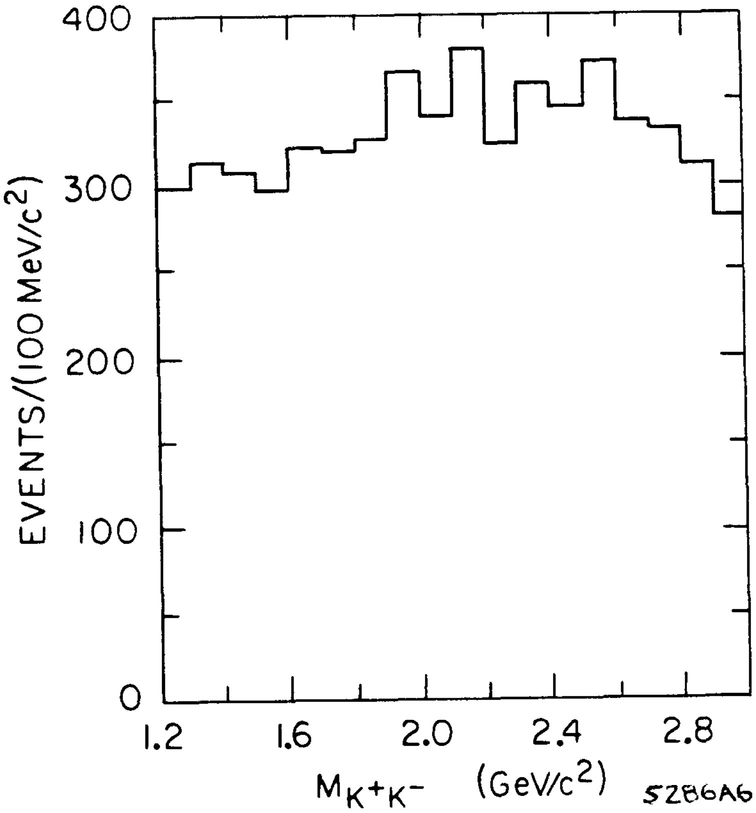
400
300
200
100
0
EVENTS/(100 MeV/c2)
1.2
1.6
2.0
2.4
2.8
MK+K- (GeV/c2)
5286A6

Fig. 7

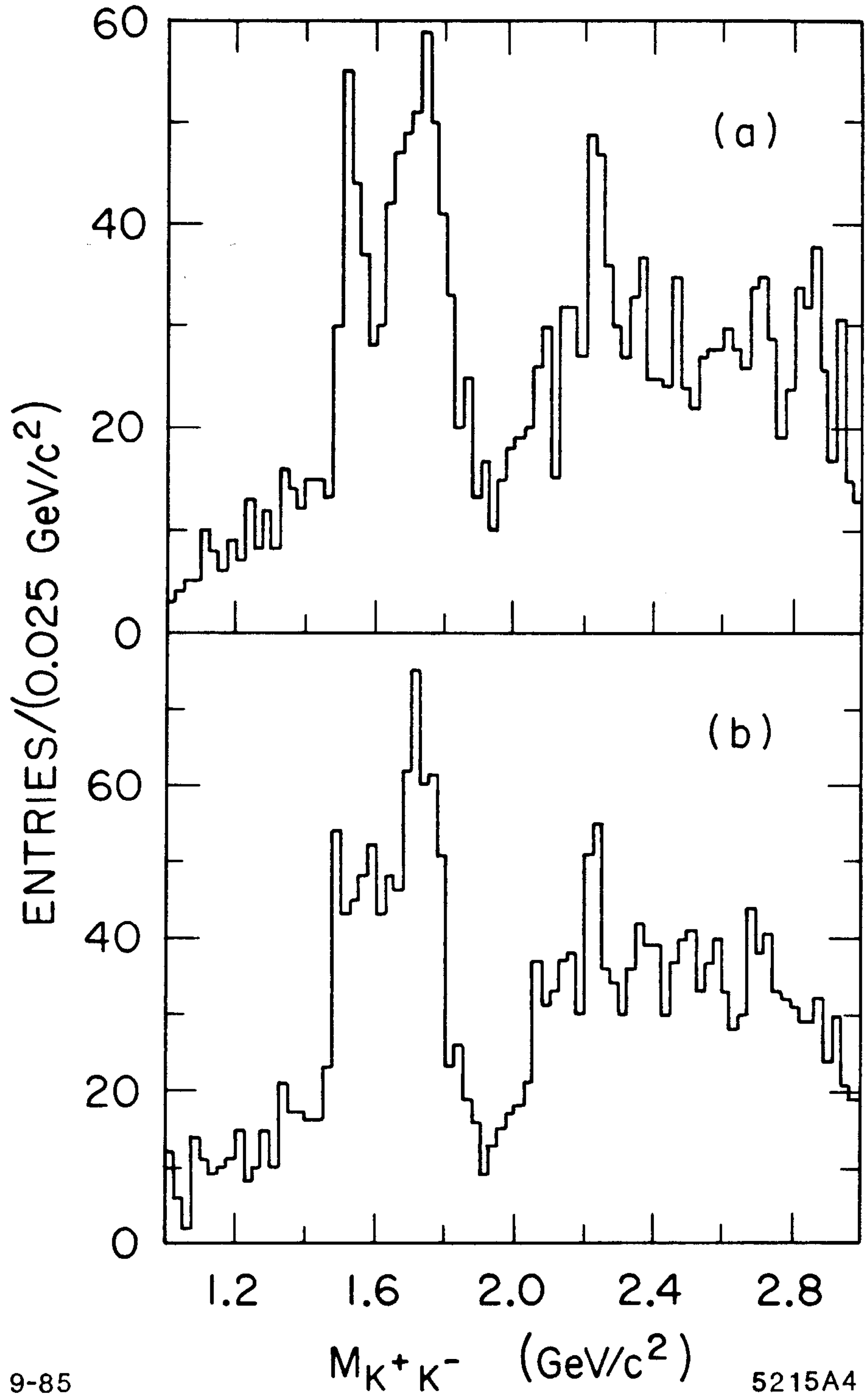
ENTRIES/(0.025 GeV/c²)
(a)
(b)
0
20
40
60
1.2
1.6
2.0
2.4
2.8
M_{K⁺K⁻} (GeV/c²)
9-85
5215A4

Fig. 8

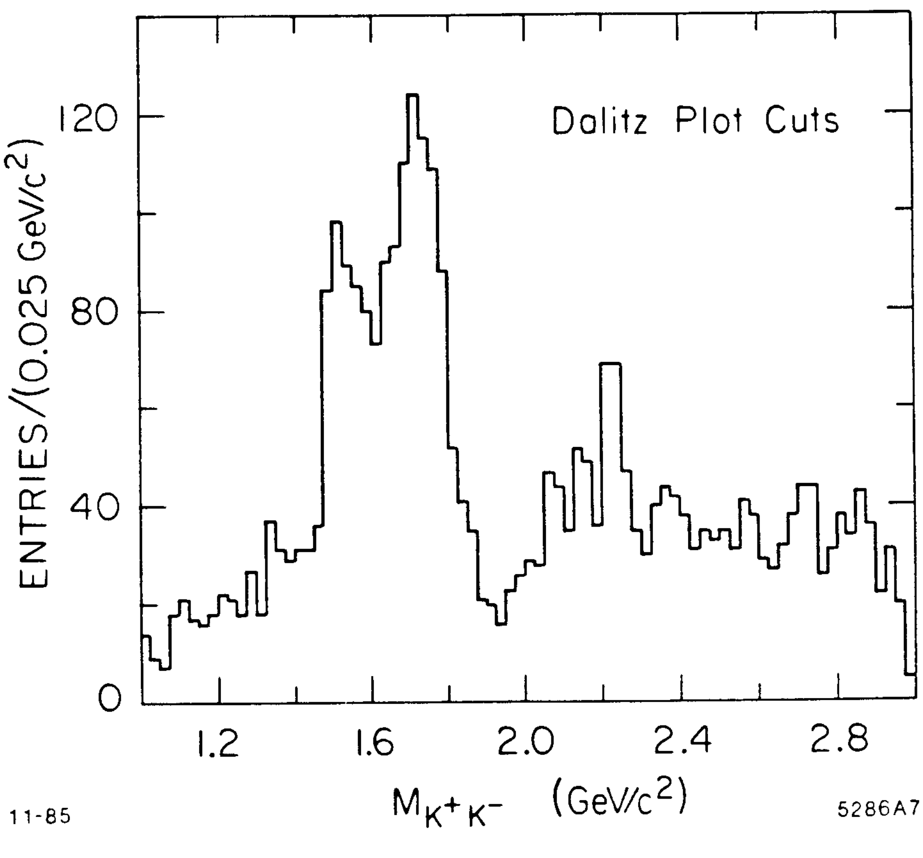
120
80
40
0
ENTRIES/(0.025 GeV/c²)
Dalitz Plot Cuts
1.2
1.6
2.0
2.4
2.8
M K+K- (GeV/c²)
11-85
5286A7

Fig. 9